

Saltwater intrusion of the Costa de Hermosillo aquifer, Sonora, Mexico: A numerical simulation

Flores-Márquez, E. L., J. O. Campos-Enríquez, R. E. Chávez-Segura and J. A. Castro-García
Instituto de Geofísica, UNAM, México, D.F., México.

Received: November 21, 1997; accepted: February 8, 1998.

RESUMEN

La inversión de datos gravimétricos nos permitió obtener la topografía del basamento del acuífero de Costa de Hermosillo. La profundidad del basamento es compleja y varía entre 300 y 3500 m, caracterizado por alternancias de horsts y grabens. Entre la ciudad de Hermosillo y Bahía Kino se presenta un alto con una estructura semicircular. Muchos de los grabens están interconectados, sirviendo de canales para el agua de mar que fluye hacia el continente, mientras que los horsts actúan como barreras para este flujo. La forma que presentan las isóneas de sólidos totales disueltos permite avalar estas hipótesis. Los datos gravimétricos nos permitieron también establecer la existencia de lineamientos que se correlacionan con la prolongación hacia el sur de la falla de Cerro Prieto y con el lineamiento del margen del Cratón. De acuerdo con la distribución de resistividades eléctricas en el área, el frente del agua de mar se extiende por más de 25 km dentro del continente y tiene una profundidad superior a los 200 m. Basándonos en estos resultados y en los datos de pozos, reconstruimos la estratigrafía del acuífero. La información geofísica, geológica y geohidrológica se utilizó para inferir un modelo geológico del acuífero de Costa de Hermosillo, que posteriormente permitió construir secciones bidimensionales para realizar los modelos numéricos de la intrusión salina. Esta modelación se realizó con base en un tratamiento adimensional de las ecuaciones de Darcy, de continuidad para el agua y para la sal, y en una relación constitutiva entre el agua y la concentración de sales. El sistema de ecuaciones adimensionales resultante fue resuelto en dos dimensiones mediante un método de diferencias finitas, en perfiles seleccionados sobre el modelo geológico de la zona.

En donde no existen barreras para el flujo de agua de mar se observan, en los modelos, patrones advectivos de circulación de los fluidos. Sin embargo, en las porciones separadas por intrusivos o horsts se observan celdas convectivas. El flujo en el acuífero es complicado debido a la diversidad de materiales en el relleno sedimentario y a la sobreexplotación del mismo. Se tomó como condición de frontera el régimen de explotación actual y se realizaron simulaciones numéricas de circulación de fluidos hasta que el sistema alcanza un estado estacionario. Los valores de concentración de sales así obtenidos reproducen de manera aceptable los valores observados.

PALABRAS CLAVE: Geohidrología, resistividad eléctrica, gravimetría, inversión, modelo numérico, intrusión de agua salada, advección y convección.

ABSTRACT

Inversion of gravity data enabled us to obtain the basement topography of the Costa de Hermosillo aquifer. The depth to the basement ranges from 300 to 3500 m, and has a complex character. Between Hermosillo and Kino Bay, the basement constitutes a subcircular structural high. Around this structural high basement is characterized by a series of horsts and grabens. Several grabens are interconnected, allowing the flow of seawater inland. The horsts act as barriers to the seawater flow. The pattern of total dissolved solids in groundwater supports this interpretation. Gravity data also suggest the existence of tectonic lineaments correlating with the southward prolongation of the Cerro Prieto fault, and with the Craton margin lineament. From electrical resistivity distribution the seawater front extends inland more than 25 km and is more than 200 m deep. Based on borehole information and on the electrical resistivity distribution we inferred the stratigraphy of the aquifer. Geophysical, geological and geohydrological information were used to derive a geological model for the Costa de Hermosillo aquifer, which was subsequently used in a 2-D numerical simulation of salt water intrusion. A non-dimensional formulation based in the equations of Darcy, of continuity (for the water and for the salt, respectively) and in a constitutive relation (fluid density and salt concentration), was used to simulate the seawater intrusion. The resulting equations were solved, through a finite difference scheme, for the parametrized geologic model along selected profiles.

We find an advective pattern where no barrier exists to the seawater flow. However, those sections separated by intrusives or horsts show convective cells. The aquifer flow is complicated by the changing nature of the sedimentary infill and the over-exploitation of the aquifer in the zone. Assuming the present rate of withdrawal the steady-state simulated reproduces salt concentration agrees with the observed values.

KEY WORDS: Hydrology, electrical resistivity, gravimetry, inversion, numerical model, saltwater intrusion, advection and convection.

INTRODUCTION

Hermosillo, Sonora is located near the coast of the Gulf of California (Figure 1). The area between the coast and Hermosillo is to be called the Costa de Hermosillo. It is one of the most important agricultural districts of Mexico. The exploitation of coastal groundwater started in 1945 with 15 wells. In 1950 there were 258 wells pumping water, and by 1955 there were 484 (Cruikshank and Chávez-Guillen, 1969). Today there are more than 550 wells in operation. This withdrawal far exceeds the natural recharge and upsets the natural balance between fresh and salt water. Severe problems of seawater intrusion are already observed in several wells. Near to the shore there are high salt concentrations, and wells must be abandoned. As this aquifer represents the only source of irrigation water, the size of the irrigation areas is diminishing.

A study of the evolution of the aquifer began with piezometric, chemical and pumping test thirty years ago by the National Water Commission (CNA, Comisión Nacional del Agua). Due to the over-exploitation, the position of the salt-water front advanced from 5 km in the 60's to more than 30 km inland in 1996 (Figure 2). The observed potentiometric surface was lowered at the rate of 1 to 2 m per year during that period. Thus, the depth to the potentiometric surface increased from 15 m in the 60's to 125 m in 1994 (Figure 3). The rational administration of this coastal aquifer requires a detailed knowledge of the hydrogeologic system to be able

to numerically simulate the seawater intrusion under several extraction regimes to define the most rational exploitation approach. In particular this numerical simulation would allow one to establish the actual pattern of fluid circulation.

An upper and lower aquifer constitute the coastal hydrogeologic system of the Valley of Hermosillo. These two aquifers are separated by a clay layer.

Steinich *et al.* (1997) conducted five Schlumberger-type vertical electric soundings (VES) with interelectrode spacing, AB/2 ranging between 315 and 675 m employed along an approximately 60 km long NW-SE profile. This profile ended about 15 km inland and 20 km southwest of Hermosillo. The second profile intersects perpendicularly the previous one including three VES.

They were able to establish the structure of the unsaturated (vadose) zone and of upper portion of the aquifer. In particular, they infer that the upper and lower aquifers merged south of Hermosillo. They suggested that the low-quality water near Hermosillo and Miguel Alemán was due to irrigation with brackish groundwater from seawater intrusions and with untreated sewage.

In general, the problem of seawater intrusion analysis is formulated in terms of the fluid flow and mass transport equations. In the last decades numerical schemes have been developed to solve the resulting nonlinear differential equa-

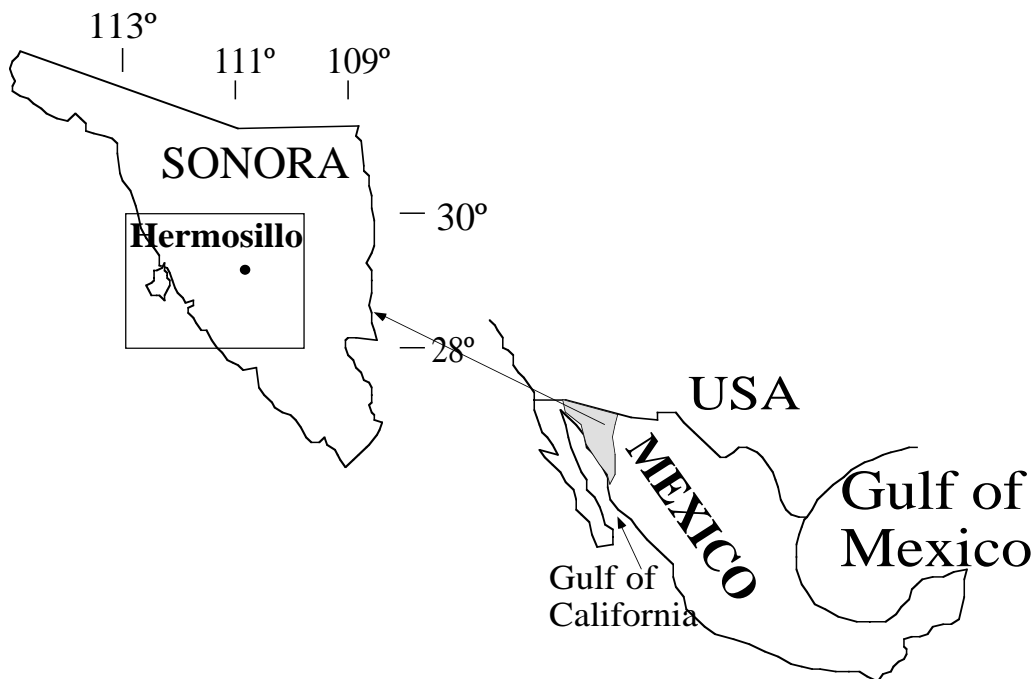


Fig. 1. Location of the Costa de Hermosillo zone.

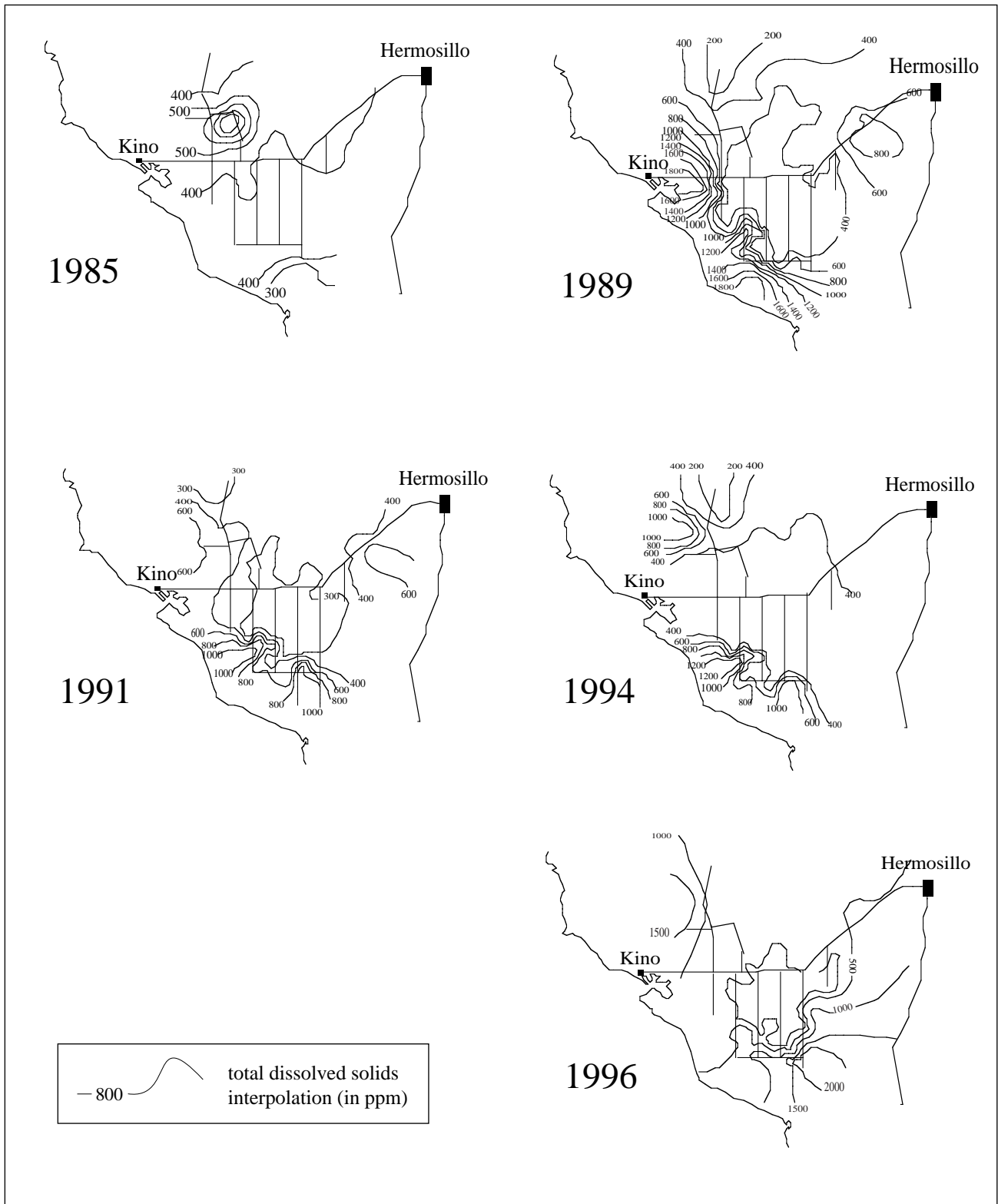


Fig. 2. Evolution of total dissolved solids (contours in ppm) of the Costa de Hermosillo aquifer from 1985 until 1996. Original data were provided by Distrito de Riego No. 51 of the Comisión Nacional del Agua (CNA).

tions. The approaches depend on: (i) the kind of interface of the seawater front that is assumed (sharp or fuzzy); (ii) the type of cross-section (horizontal or vertical); (iii) the time

regime (transient or steady-state); and (iv) the kind of numerical solution scheme (finite elements, finite differences, etc.). Examples of this research conducted in the past are

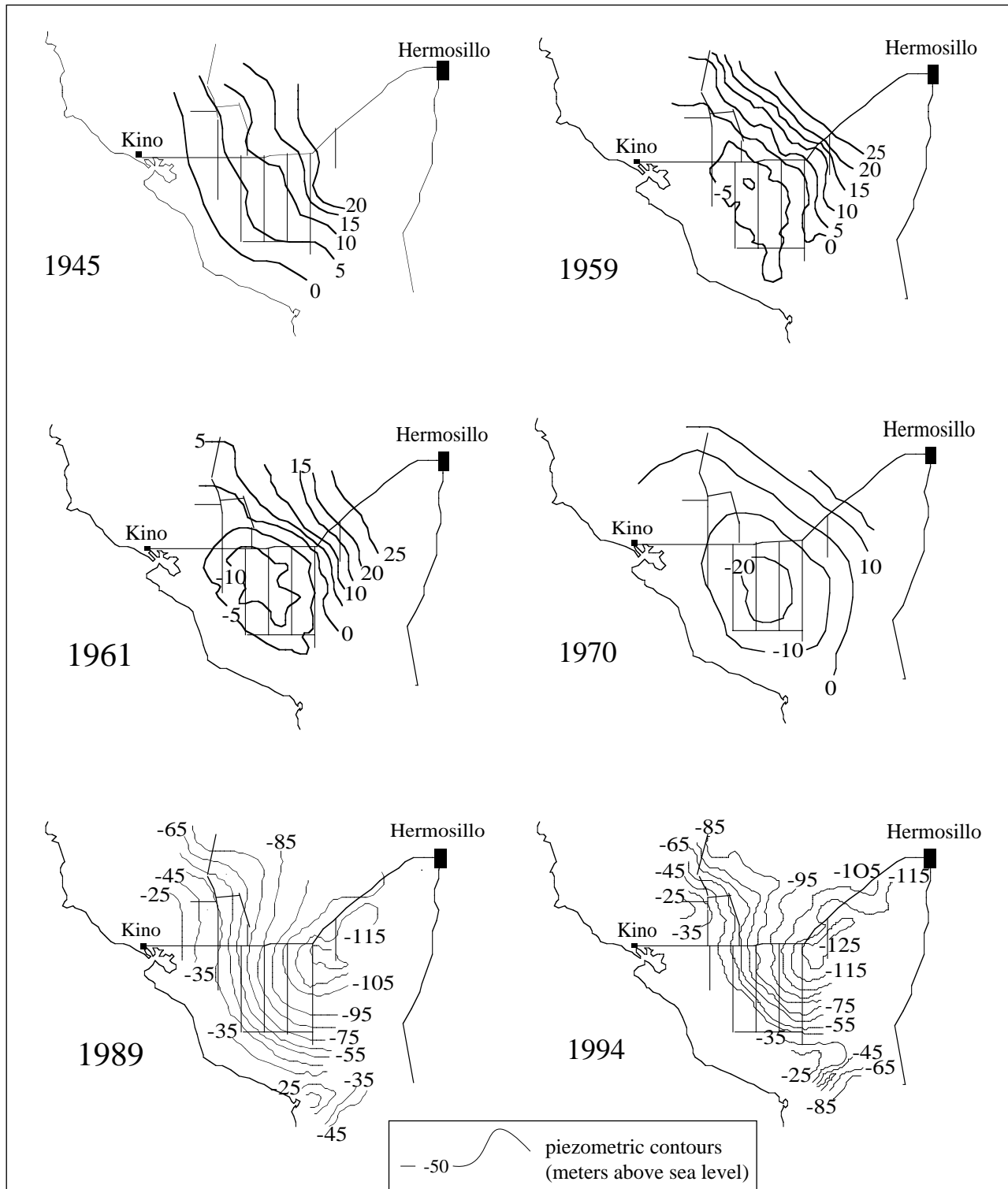


Fig. 3. Evolution of potentiometric surface, contours in meters of the Costa de Hermosillo aquifer from 1945 until 1994. Original data from Cruickshank and Chávez-Guillén (1969), and data provided by Distrito de Riego No. 51 of the Comisión Nacional del Agua (CNA).

Bear and Dagan (1964) and Shamir and Dagan (1971) who reported solutions based on a sharp interface assumption; Mualem and Bear (1974) discussed the effect of a discontinuous stratification on the shape of the interface; Henry (1959,

1964) developed the first analytical solution including dispersion; Pinder and Cooper (1970) used the method of characteristics to solve the convective-dispersive transport equation with a constant dispersion coefficient; Lee and Cheng

(1974) used a stream function to obtain a steady-state solution; and more recently, Segol *et al.* (1975) and Segol and Pinder (1976) used finite elements to solve the transport equation. They took into account a velocity-dependent dispersion. In most of the cases the integration of geological and geophysical information has not been considered.

The first objective of this extensive multidisciplinary study is to characterize the geohydrological system in terms of a geological model for the Costa de Hermosillo aquifer. The second objective is to analyze the seawater intrusion into the aquifer. A distinctive feature of the present work is that we have integrated geophysical, geological, borehole and geohydrological information. That enabled us to characterize the geological units constituting the aquifer. The basement topography was obtained from inversion of gravity data. We find in particular that the basement is affected by regional lineaments correlating with the NW-SE Cerro Prieto fault. Vertical electric soundings proved useful in defining the front of the seawater intrusion, and to infer the stratigraphy of the geological sequence.

Our geologic model was next used to numerically simulate the seawater intrusion in the aquifer. The problem is formulated in terms of the Darcy equation, the fluid continuity equation and the mass continuity equation (Flores-Márquez, 1992). The resulting nonlinear differential equations are solved by a finite difference method. We performed 2-D numerical simulations of salt water intrusion in the region to obtain the fluid flow and the concentrations of total dissolved solids in all parts of the aquifer.

STRUCTURAL SETTING

Gastil and Krummenacher (1977) divide the coast of Sonora between Puerto Lobos and Bahía Kino into four structural and petrographic subprovinces: the inland subprovince of unmetamorphosed upper Precambrian and Cambrian rocks resting on older Precambrian gneiss, and three other subprovinces of Cenozoic volcanic units resting on metamorphosed strata of Cambrian and later age intruded by granitic rocks of Mesozoic age (Figure 4). One of the latter subprovinces comprises Basin and Range faulted blocks; the second has north-west trending strike-slip faults, and the third, Isla Tiburón, comprises structures related to the Neogene extension of the Gulf of California basin.

The inland subprovince is bounded to the southwest by a lineament that may represent a fault of Mesozoic or possibly early Cenozoic age. There are remnants of Mesozoic marine strata intruded by Cretaceous and early Cenozoic granitic rocks (Beauvais and Stump, 1976).

The other three subprovinces have similar petrographic characteristics but they are structurally different. The base-

ment consists of Cretaceous granitic rocks emplaced in a volcanoclastic sequence of Mesozoic or late Paleozoic age. There are exposures of quartzite and carbonated rocks that may be remnants of the upper Precambrian and Cambrian terrane found to the north-east of the studied area. In all these three subprovinces, the Mesozoic formations are cut by swarms of late Cretaceous dikes and are overlain by coarse clastic and volcanic strata of middle to late Cenozoic age (Gastil and Krummenacher, 1977).

The southward prolongation of the northwest trending strike-slip fault cutting through the Cerro Prieto geothermal site (south of Mexicali City), constitutes a conspicuous regional feature. The Cerro Prieto fault extends into the Gulf of California east of the Colorado River (Gastil and Krummenacher, 1977). The southward projection of this lineament intersects the coast of Sonora near Puerto Libertad (Figure 4), and bounds subprovinces two and three, as the Sierra Noche Buena and Libertad fault in the study area. Merriam (1972) found other lineaments and faults (i.e., Arroyo Noriega faults) extending deep into Sonora, with subparallel trend to the San Andreas fault. The combination of northwest-trending strike-slip and northeast-trending normal faults is attributed to extensional tectonism related to the formation of the Gulf of California over the past 10 Ma (Gastil and Krummenacher, 1977).

STRATIGRAPHY

The study area contains steep ranges separated by wide valleys that feature intermitted drainage. Along the coast between Puerto Lobos and Kino Bay there are extensive exposures of rocks of pre-Cenozoic age. The principal outcrops are sedimentary and igneous rocks, and some metamorphic rocks. The age of rocks ranges from Precambrian to Cenozoic. A simplified description of the stratigraphic sequence follows (Figure 5).

The metamorphic basement is derived from igneous and sedimentary rocks of early Proterozoic age (Anderson and Silver, 1977; 1981). Next there is a sequence of quartzites and dolomite of late Proterozoic age. The Paleozoic sequence is exposed in several localities of Sonora: it is mainly composed by sandstones and platform limestones (Rangin, 1978).

Late Triassic - Early Jurassic continental sedimentary rocks rest on the Paleozoic sequence. A fine clastic sequence with levels of coal and limestones is exposed to the south-east of Hermosillo, deposited in lacustrine environments. This sequence was described as the Barranca Group by Alencaster (1961). The Jurassic in Sonora is characterized by the development of a northwest-southeast magmatic arc, of andesitic composition, sometimes associated with sedimentary rocks. U-Pb dates reported by Anderson and Silver (1977) range from 150 to 180 Ma. The lower Cretaceous is formed

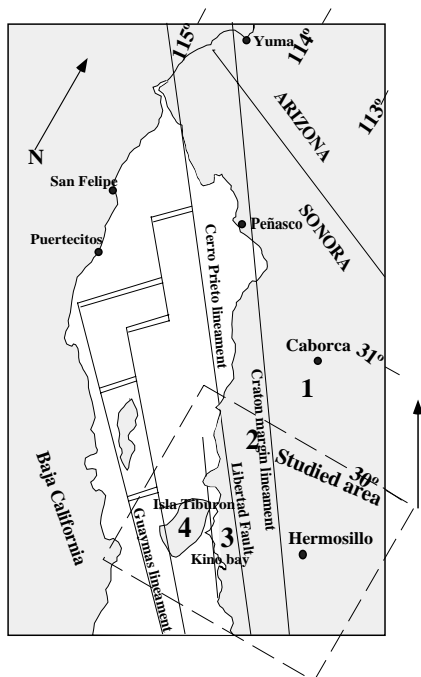
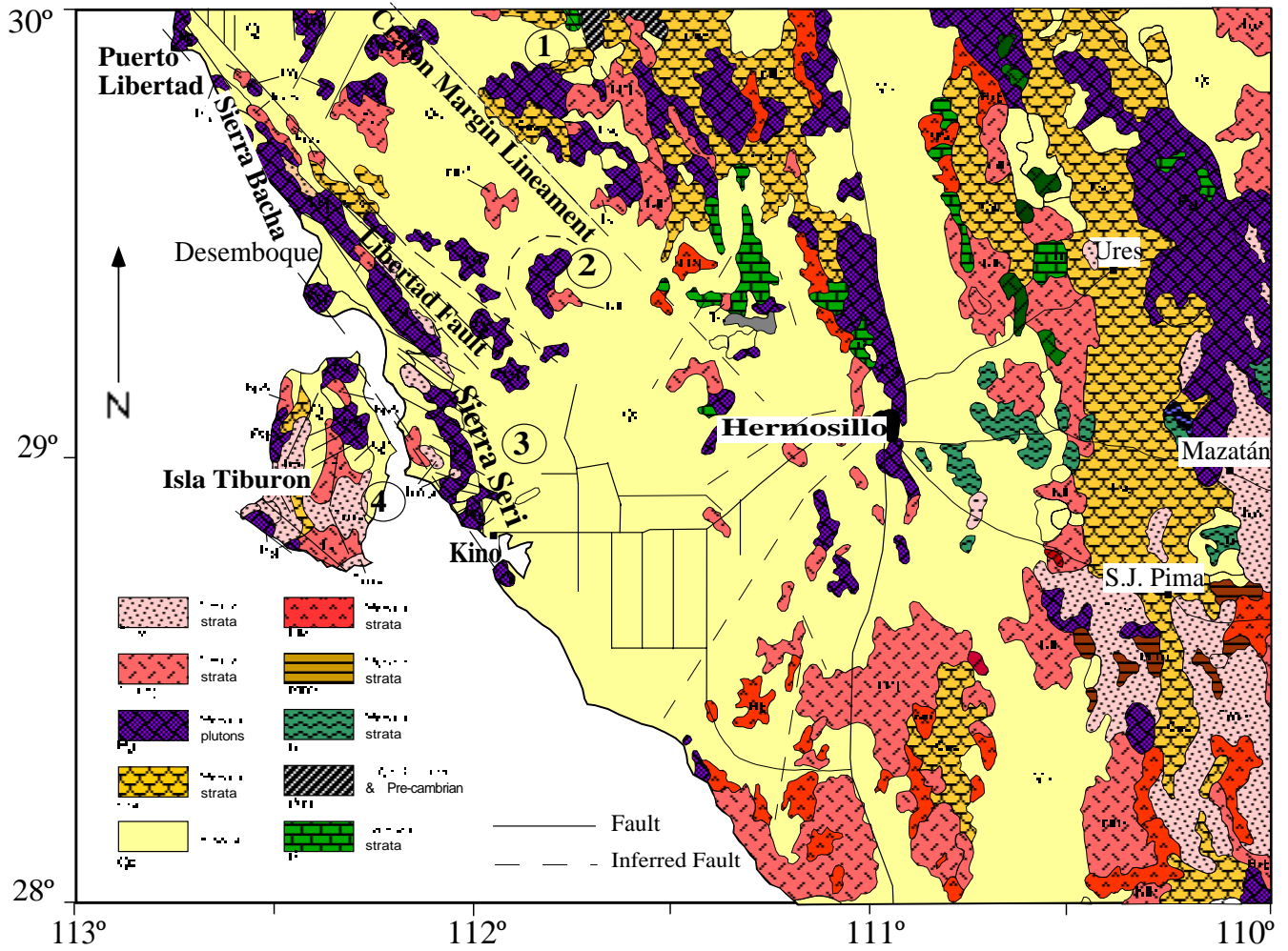


Fig. 4. Geological map indicating regional tectonic framework in the studied area, main tectonic framework between Puerto Lobos and Kino Bay were taken from Gastil and Krummenacher (1977). The structural-petrographic provinces are: 1, Precambrian basement; 2, Mesozoic basement with basin and range type faulting; 3, Mesozoic basement with predominantly northwest-trending strike-slip faulting; 4, Isla Tiburón related to the Gulf of California spreading-transform system.

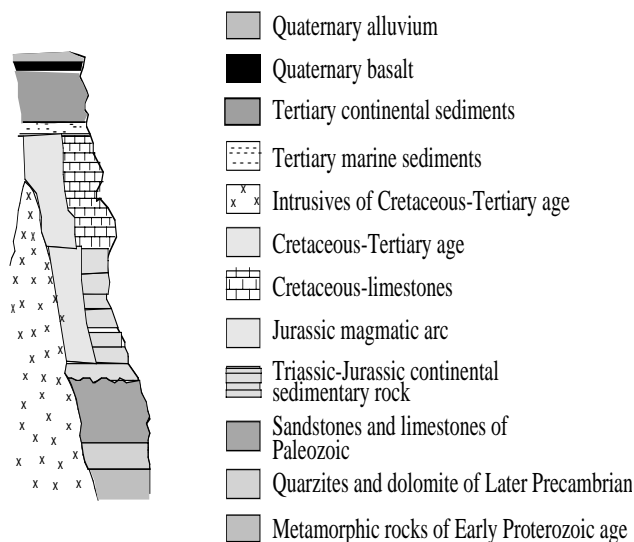


Fig. 5. Schematic stratigraphic section of western Sonora.

by andesitic flows associated with marine sediments, in central and western Sonora, or by marine limestones in the eastern part of the State. In the Late Cretaceous the State of Sonora was affected by compressional tectonic processes and by granitic intrusions accompanied by andesitic lava flows (Rangin, 1981). The pyroclastic and andesitic flow are described by King (1939) as the Lista Blanca Formation.

Two Tertiary volcanic sequences cover the old rocks in Sonora. A lower sequence is composed of andesitic flows (mainly present in the southern portion of the State), whereas the upper one comprises acid tuffs. During the Neogene the western part of Sonora was affected by normal faulting with NW-SE trends. These events produced basin-and-range structures filled with Tertiary continental sediments. Fluviodeltaic deposits are found along the coast. These deposits are composed of sand, silt and gravel. Several boreholes drilled by Recursos Hidráulicos (Gómez, 1971) cut Miocene to Holocene marine sedimentary strata, presumably deposited between the ranges (Gastil and Krummenacher, 1977).

The coastal hydrogeologic system of the Valley of Hermosillo consists of two interconnected aquifers. The upper aquifer contains silt, sand and gravel from Miocene to Recent age and is approximately 200 m thick (Andrews, 1981). A thick fossiliferous marine clay, interbedded with silt and sand, called the Blue Clay (Arreguín *et al.*, 1968) separates the upper aquifer from the lower one. The thickness of the lower aquifer ranges between 22 m and 280 m. The lower aquifer contains Late Mesozoic clastics and volcanic rocks (Andrews, 1981).

GRAVITY DATA

The sub-surface structure of the study area was inferred

from available Bouguer gravity data (De la Fuente *et al.*, 1994) and by our gravity observations along five profiles (Figure 6). We used a SCINTREX μ Gal type gravity meter. The gravity survey was tied to the International Gravity Standardization Net 1971 (IGSN71) (Woollard, 1979) through the gravity base located at Hermosillo international airport. Topographic control was obtained by first order leveling. The Bouguer anomaly was computed with a density of $2,670 \text{ kg/m}^3$, and was referred to sea level. The Bouguer anomaly has a complex pattern (Figure 7). We observe two groups of lineaments. The first group has a conspicuous NE-SW orientation and is found to the south and west of Hermosillo. East and north of this city the lineaments have a mean N-S trend. These two sub-groups of lineaments correlate with surficial mapped faults and with the main trends of the geology (Sierra Horcasitas, Sierra Juvenal, Sierra Espinazo Prieto).

The second group of lineaments which has a mean NW-SE direction includes the Libertad fault or southward continuation of the Cerro Prieto fault, and the Craton-Margin lineament. Both systems conform a series of horsts and grabens trending perpendicular to the coast. Between Hermosillo and Kino Bay there is a sub-circular gravity high composed of three large anomalies and two minor ones. The grabens end against the craton-margin lineament. East of Hermosillo a broad graben extends into the first geologic subprovince of Gastil and Krummenacher (1977), where it turns to N-S. Presentation of the Bouguer anomaly as a digital image enhances the above mentioned features. Figure 8 was obtained by convolving the Bouguer anomaly image with a Mexican hat-shaped operator, and with a sharp-edge enhancing operator. Note the steep gravity gradients with a semicircular shape over the eastern part of the region, which may reflect a boundary in the density and lithology of the crystalline basement.

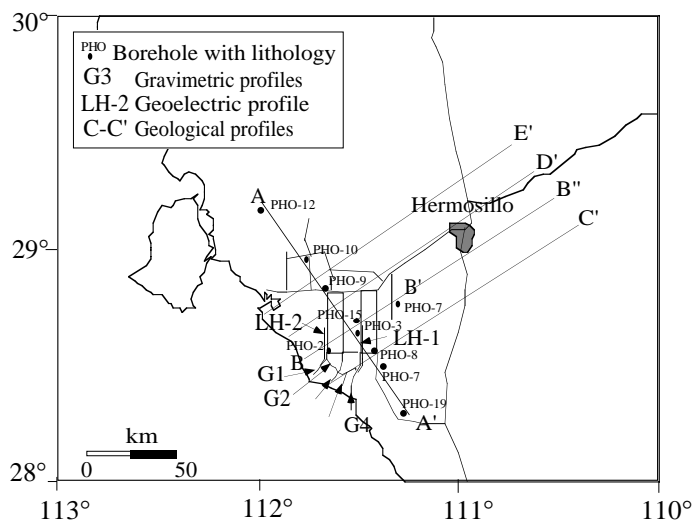


Fig. 6. a) Location of geophysical and model profiles of the Costa de Hermosillo zone.

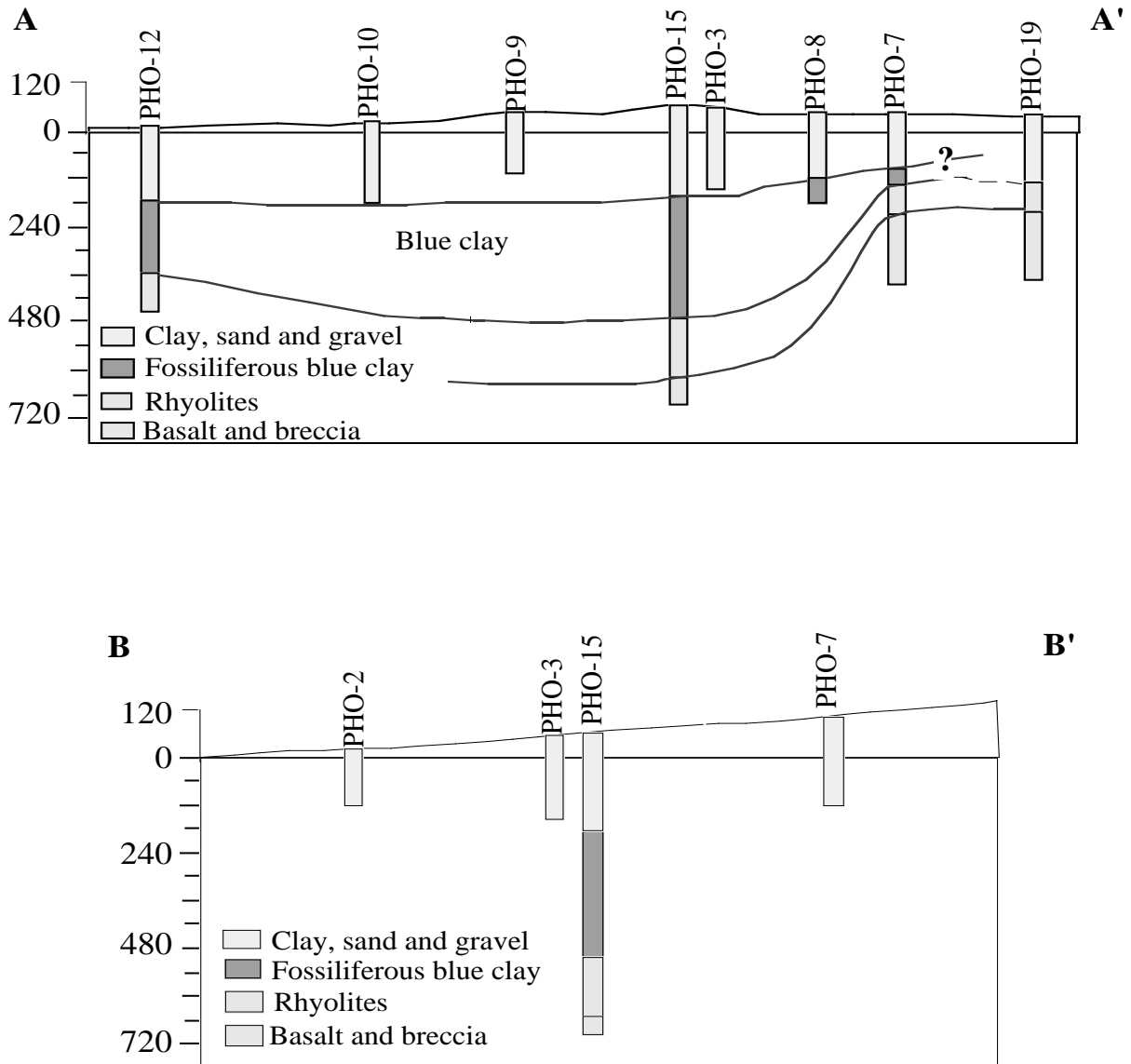


Fig. 6. b) Lithological profiles based on borehole information.

The high-frequency part of the power spectrum associated with shallow gravity sources is assumed to represent the residual anomaly (Figure 9). A low-pass filter with a cut-off frequency of 0.78 cycles/km was used for the regional-residual separation. The residual gravity anomaly shows basically the same pattern as the Bouguer anomaly (Figure 10). The basement topography was obtained by inverting the residual gravity anomaly following Pilkington and Crossley (1986). The inversion method assumes a layered model of constant density contrast bounded by a horizontal plane $z=0$, and a surface $z=h(r)$ defining the basement topography. The function $h(r)$ yields the basement topography with respect to some mean level $z=z_0$. The gravity effect is (Grant and West, 1965) :

$$\Delta g(x, y) \equiv -G\Delta\rho z_0 \int_{-\infty}^{\infty} \int_{-\infty}^{\infty} h(x', y') \frac{dx' dy'}{\left[(x-x')^2 + (y-y')^2 + z_0^2 \right]^{3/2}} \quad (1)$$

Parker (1973) formulated the solution as a forward problem in the frequency domain, thus:

$$\Delta \hat{g}(\mathbf{K}) = -2\pi G\Delta\rho e^{-|\mathbf{K}|z_0} \sum_{n=1}^{\infty} \frac{|\mathbf{K}|^{n-1}}{n!} \hat{h}(\mathbf{K}) \quad (2)$$

where $\Delta \hat{g}(\mathbf{K})$ and $\hat{h}(\mathbf{K})$ are the Fourier transforms of the gravity data and of the basement topography $h(r)$. Pilkington and Crossley (1986) showed that the $n=1$ term represents a good first estimate, and can be used to linearize the forward problem such that:

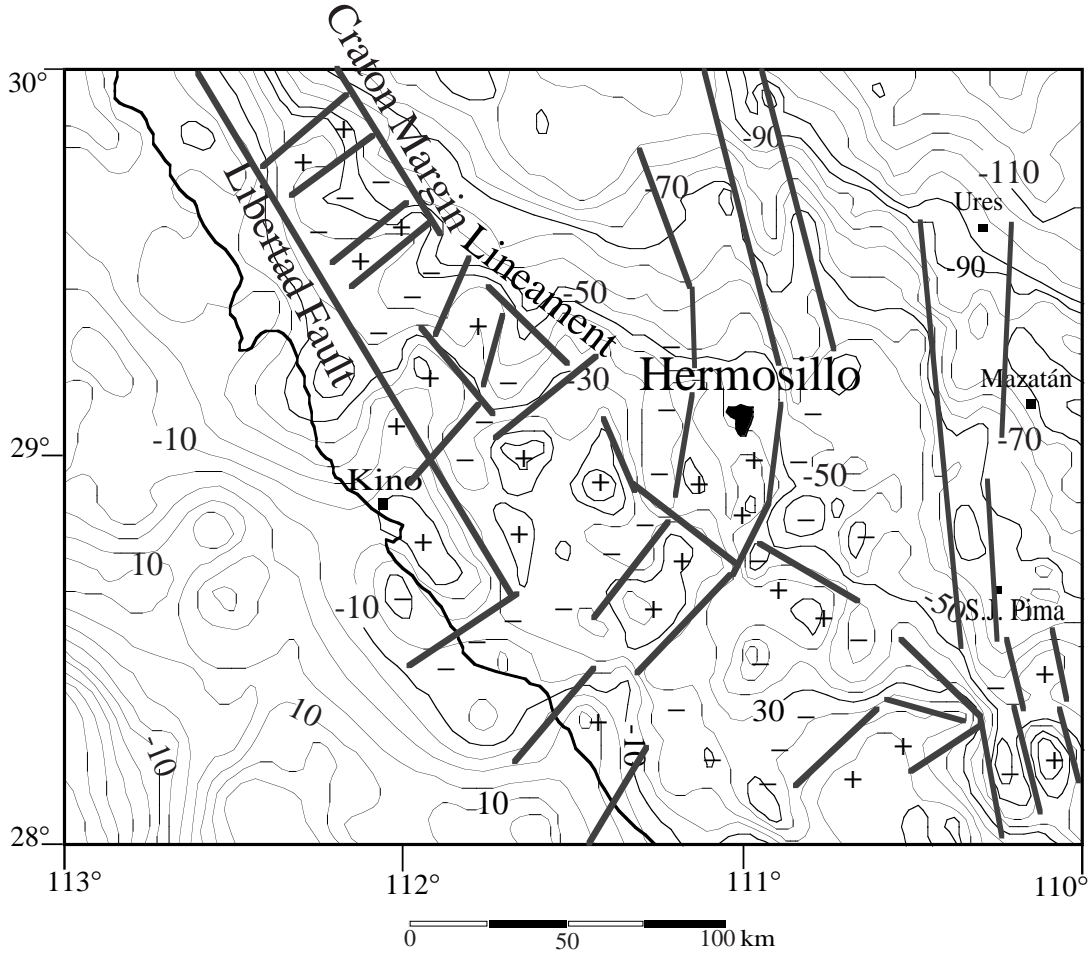


Fig. 7. Bouguer anomaly map of the studied area (gravity data from De la Fuente *et al.*, 1994) including interpreted lineaments, (+) structural highs, and (-) structural lows. Main tectonic lineaments are also indicated by dashed lines.

$$\Delta\hat{g}(\mathbf{K}) = \mathbf{F}^{-1} \left\{ -2\pi G \Delta\rho e^{-\mathbf{K}|z_0} \mathbf{F}[h_0(\mathbf{K})] \right\}. \quad (3)$$

Abdoh *et al.* (1990) restated equation (3) in matrix form as $\mathbf{g} = \mathbf{F}^* \mathbf{T} \mathbf{F} \mathbf{h}$, \mathbf{F} is the Discrete Fourier Transform and \mathbf{T} is a diagonal matrix with $t_i = -2\pi G \Delta\rho e^{-\mathbf{K}|z_0}$. This is equivalent to a singular value decomposition, where \mathbf{F}^* and \mathbf{F} represent eigenvector matrices, and \mathbf{T} contains the eigenvalues t_i . To invert for the topography, an iterative scheme can be designed as:

$$\mathbf{h}_{n+1} = \mathbf{h}_n + \mathbf{F}^* \mathbf{T}^{-1} \mathbf{F} (\mathbf{g}_{\text{obs}} - \mathbf{g}_n). \quad (4)$$

A constant can be added to small eigenvalues to avoid instabilities that arise from small t_i , corresponding to large wavenumbers. Pilkington and Crossley (1986) discussed the convergence of the solution, and they investigated the behavior of the eigenvalues for different contrast densities and reference depths.

The inversion was constrained by using a density contrast of 480 kg/m^3 and a reference depth of 2 km. These pa-

rameters were obtained once a series of inversions has been computed. The final result does not depend on these values; however, there will be instabilities in the short-wavelength features of the buried topography due to small eigenvalues, directly related to the value of z_0 . The value we choose for z_0 minimizes these instabilities.

The depth to basement ranges from 300 to 3500 m (Figure 11). Between Hermosillo and Kino Bay, the basement is shallower, with depths between 300 and 2500 m. The basement deepens around the edges of the structural high. (1) To the E and N of Hermosillo, we find lineaments of N-S direction; (2) in the second and third geologic subprovinces the lineaments have a NE-SW orientation; (3) in these same domains we also observe NW-SE lineaments as discussed by Gastil and Krummenacher (1977) which they related to the opening of Gulf of California. A series of alternating structural highs and lows characterize the basement in the study area. Several of the structural lows are connected so that flow of seawater can occur. The possible flow paths are indicated in Figure 8. On the other hand, the top of the subcircular

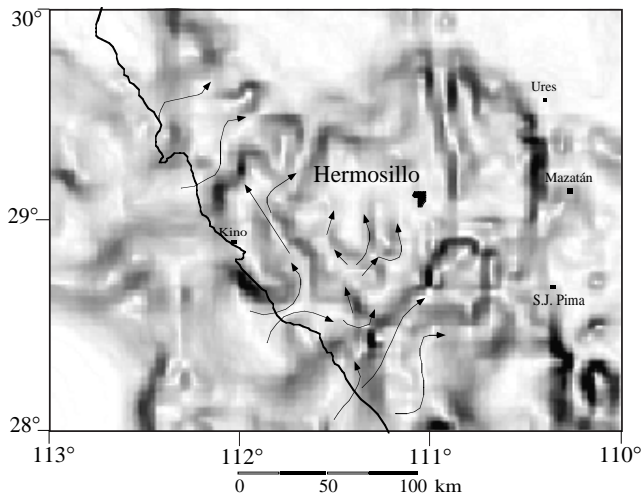


Fig. 8. Bouguer anomaly map displayed as image. It has been convolved with a Mexican hat-shape filter, and an edge sharpen operator. Location of geologic cross sections is indicated. Possible flow paths for the seawater intrusion are also indicated by arrows.

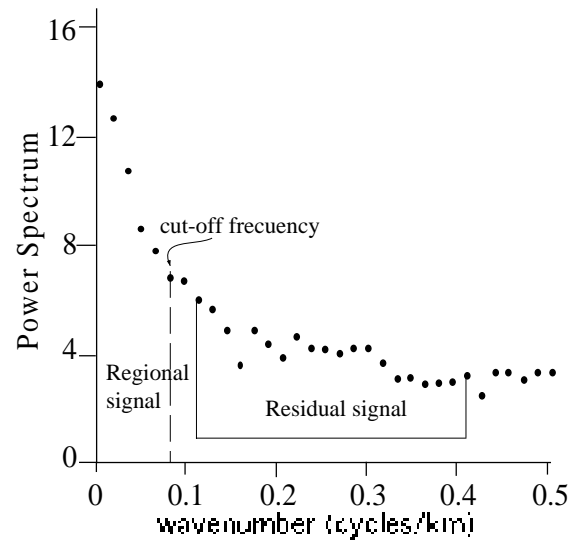


Fig. 9. Power spectrum of the Bouguer anomaly. Cut off frequency is 0.781 cycles/km. The second domain (high frequency content) is associated with the residual anomaly.

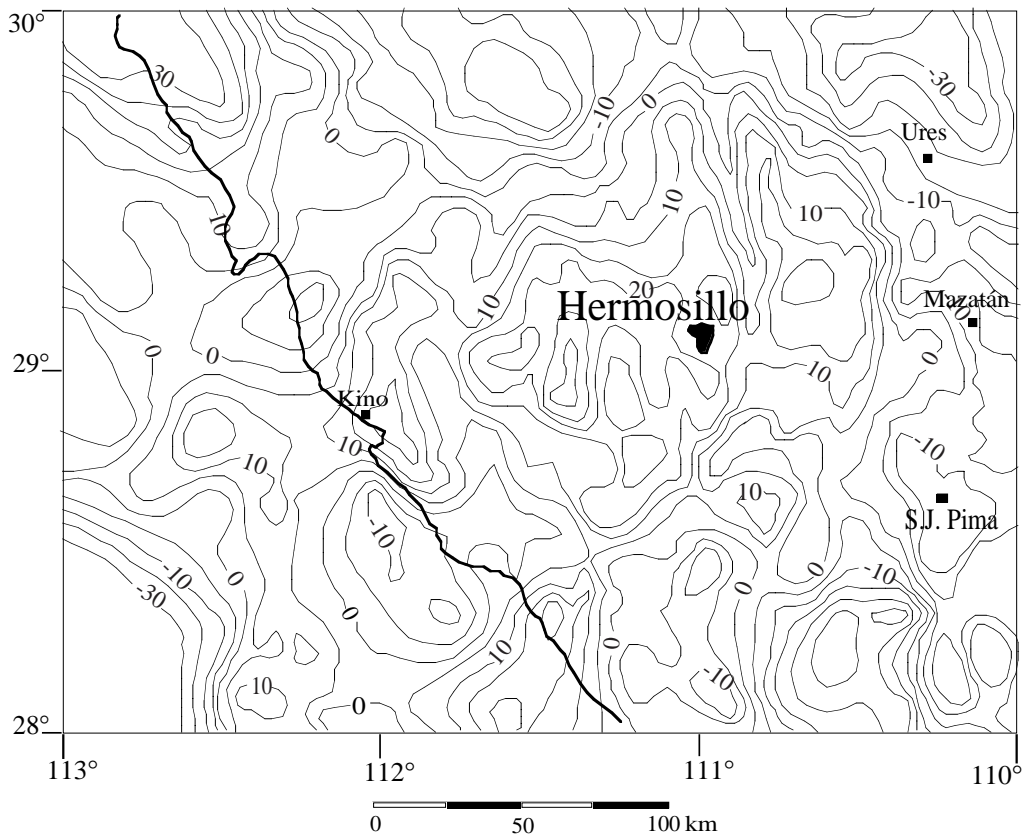


Fig. 10. Residual anomaly. Contour interval is 5 mGal.

structural high may act as barrier to the seawater flow. The pattern of total dissolved solids in this area (Figure 2) shows that the highest part of the structural high has the lowest concentration of total dissolved solids, thus supporting the present interpretation on the regional circulation of seawater.

RESISTIVITY DATA

Twenty vertical electric soundings (VES) were distributed along profiles LH-1 and LH-2 (Figure 6a). A Schlumberger array was used with interelectrode spacing, $AB/2$,

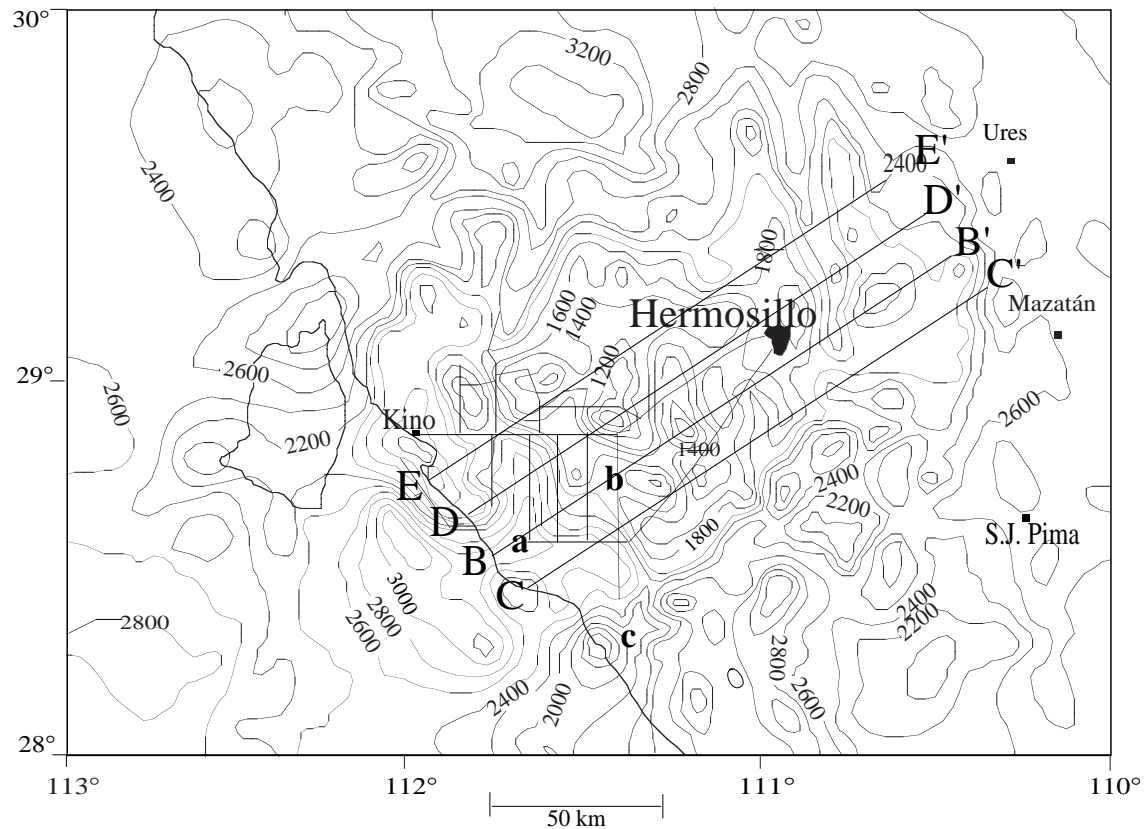


Fig. 11. Basement topography. Contour interval is 200 m. a, b, c represent main tectonic depressions.

of up 1000 m. We used a 2.5 kW IPC7 transmitter and a IPR-10A receiver, by SCINTREX. Figures 12 and 13 show the resistivity sections and their interpretations.

Figures 12a and 13a show the pseudo-resistivity distribution. In general we observe low resistivities for electrode spacings of about 5 m. Then we observe resistivities varying between 30 and 200 W-m. Finally, at the bottom we find again low resistivity values. A 1-D inversion was carried out for each of the VES using the method developed by O'Neill (1975) to calculate the real resistivities and thickness of each geoelectric bed. The maximum depth of penetration was about 200 m. The interpreted geoelectrical layers were correlated with available well logs to reduce the ambiguity in the interpretation.

According to our interpreted geoelectric section we find low resistivities at depths shallower than about 60 m. The geoelectric profile LH-1 (Figures 6 and 12) depicts a shallow region of high resistivity, which corresponds to conglomerates and sands (600-3000 W-m). Immediately below we have clay and also granular material of low resistivity values (5-30 W-m). The lower electrical layer may be saturated with saline water. The heavy line indicates the saline interface. The discontinuity in resistivity may be due to fault (Figure 12c), as it coincides with the Libertad fault (Figure 4). Re-

sistivities of 12 W-m correspond to layers of clays and limes at depths ranging between 8 and 10 m, approximately.

This result shows that the saline intrusion goes beyond the location of the geoelectric profiles, and penetrates far inland. The inferred front of the saltwater intrusion penetrates more than 25 km and is more than 200 m deep (Figures 12c and 13c). This implies that the impervious clay barrier cannot stop the seawater intrusion (that the clay layer is not continuous). Steinich *et al.* (1997) had also previously inferred that the upper and lower aquifers merge south of Hermosillo.

We integrated our gravity (basement topography, and tectonic lineaments) and geoelectric results (location of the seawater front, and electrostratification), with all the available geological information (borehole information, regional stratigraphic column, surface geology) to derive a single geological model of the Costa de Hermosillo aquifer. Figure 14 shows four geologic cross sections (see Figure 6a for location).

As we shall see below, available hydrogeological information was also incorporated into the geologic model. Subsequently we used this model to numerically simulate the seawater intrusion into the aquifer.

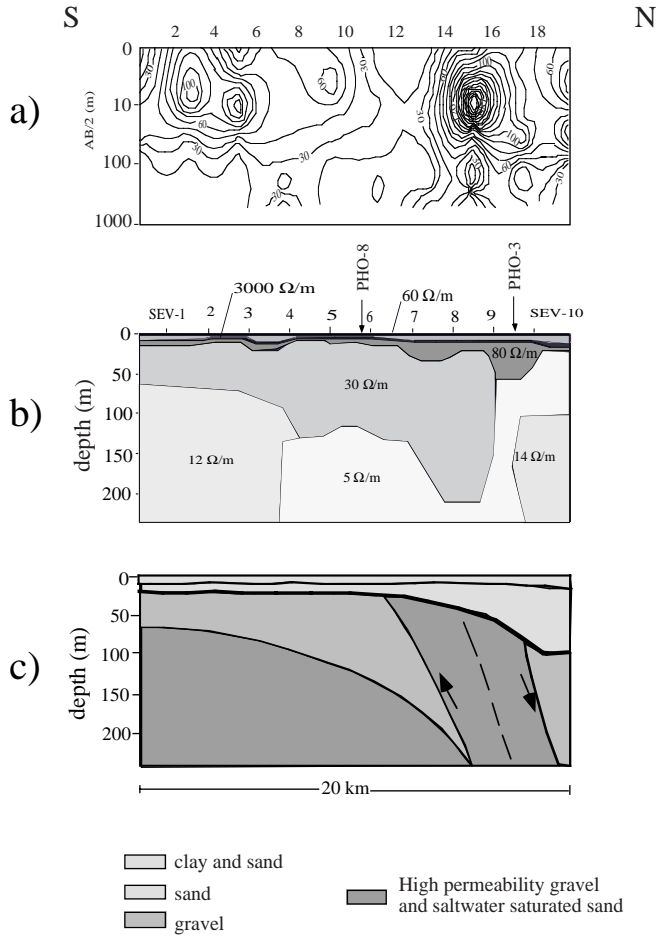


Fig. 12. Resistivity cross-section LH1. (a) apparent pseudo-resistivity section, (b) resistivity section, and (c) simplified geologic model. Resistivities are given in ohm-m. See Fig. 6a for location.

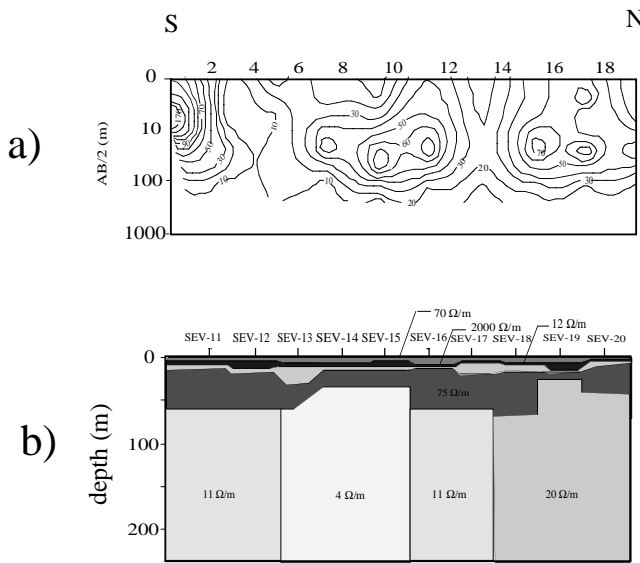


Fig. 13. Resistivity cross-section LH2. (a) apparent pseudo-resistivity section, (b) resistivity section. Resistivities are given in ohm-m. See Fig. 6a for location.

MODELING OF SEAWATER INTRUSION

The evolution of an aquifer is governed by the Darcy and the continuity equations for the fluid. In addition the seawater intrusion obeys the continuity equation for dissolved salt and the constitutive equation which relates fluid density to the concentration. (See Flores-Márquez 1992; 1998).

The general Darcy equation has the form:

$$\mathbf{q} = -\frac{\mathbf{k}}{\mu} \text{grad}(p + \rho g z) \quad (5)$$

where \mathbf{q} is the vector of flow (L/T), p is the pressure, ρ is the density (M/L³), g is the gravity acceleration (L/T²), \mathbf{k} is the permeability tensor (L²), z = distance measured along the vertical (L), and μ is the viscosity.

This equation can be expressed in terms of the stream function in a dimensionless form as:

$$\nabla \cdot [\mathbf{k} \cdot \nabla(\psi + \gamma c z)] = s \frac{\partial c}{\partial t} \quad (6)$$

where c is the relative salt concentration and γ is the constant relating the maximum density of the fluid to the reference density of the fluid ρ_0 (equivalent to fresh water) $\gamma = \frac{\rho_{\max}}{\rho_0} - 1$.

The equivalent freshwater head ψ (stream function) is defined as:

$$\psi = \frac{p}{\rho g} + z \quad (7)$$

The solute continuity equation is

$$\nabla \cdot (\mathbf{D} \cdot \nabla c) - \mathbf{q} \cdot \nabla c = \frac{\partial c}{\partial t} \quad (8)$$

where \mathbf{D} is the dispersion tensor, and \mathbf{q} is the fluid velocity (L/T).

The constitutive relationship between fluid density and concentration may be expressed as:

$$\rho = \rho_0(1 + \gamma c) \quad (9)$$

Solution of flow equations using a 2-D finite difference scheme.

The solution of the coupled Darcy and solute continuity equations was obtained with help of a finite difference scheme, based on a double iterative approach using a Gauss-Seidel over relaxation algorithm. This procedure was applied until convergence. A classical square finite difference scheme using a five-point formula within the domain and a four-point formula at the boundaries were used. This scheme enables one to take into account an heterogeneous medium, anisotropy of the physical properties, density dependence on the salt concentration and a complicated geometry for the geological model.

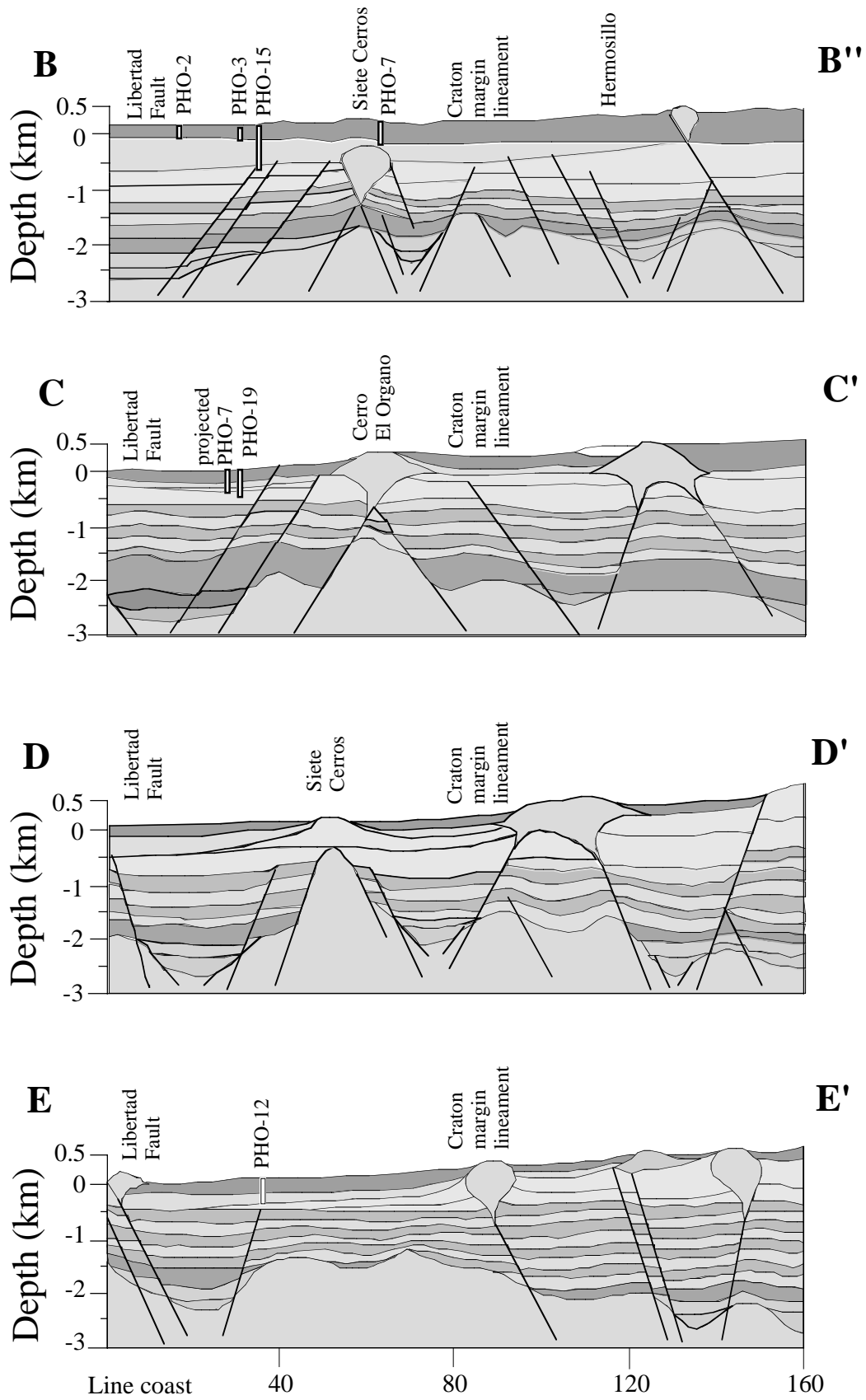


Fig. 14. Geological sections elaborated from the surficial geology, borehole information, the basement topography, and the geoelectric sections (see Fig. 5 for geological units identification).

In general the parameters necessary to carry out the numerical simulation (e.g., permeability, viscosity, etc.) change for the same geological formation from place to place. For the study area there are no direct determinations of these parameters. We inferred the value of the parameters using the known hydrologic conditions, *i.e.*, we made some trial simulations changing the values of the different parameters. The values which were most representative of the known hydrologic conditions were used in the final simulations. Table 1 shows our values assigned to permeability, porosity and dispersion coefficient of each geologic unit comprising the aquifer.

Our values are in the range of the values assigned to similar formations elsewhere (e.g., Cruickshank and Chávez-Guillén, 1969; Gipouloux *et al.*, 1991; Ferrasi and Marinelli, 1996; Ghassemi *et al.*, 1996). We assume a high permeability contrast between the basement and the volcano-sedimentary cover. The contrast between different geologic layers may be of up to two orders of magnitude.

The geology was simplified in the model, by clustering or ungrouping the geological layers as required. In general, we used five different layers. An important assumption was the high permeability of the fractured igneous rocks and the carbonate layers. The 160 x 3 km domain of each geologic section was represented by a regular grid of 120 x 30 nodes.

We took the anisotropy of hydro-physical properties of the layers into account as it strongly influences the fluid circulation.

To solve the system of equations for the specific case of the Costa de Hermosillo aquifer, we assumed: (i) a fluid with a linear density relation depending on the salt concentration change; (ii) a Boussinesq incompressible fluid, except for the buoyancy term; (iii) small filtration velocities and gradients; (iv) an anisotropic permeability tensor; (v) that fractures behave as in a high-permeability porous medium.

The boundary conditions for the salt concentration equation in our models were as follows.

At the surface and bottom of the models the salt concentration is free; this is equivalent to imposing a constant flow.

At the right limit, the value of the salt concentration is assumed to be zero (fresh water).

At the left limit, the value of salt concentration corresponds to the seawater content in the region.

The boundary conditions for the Darcy equation in term of the stream function (ψ) were as follows:

At the surface the water flow rate depends on the rainfall rate.

At the bottom the potential ψ is zero, corresponding to no water exchange with the basement.

At the lateral limits a free water flow rate is imposed, equivalent to free water interchanges.

The boundary conditions were kept constant except at the surface, where they were modified to fit the observations.

Our numerical simulation (Figures 15 to 18) shows that the impervious basement acts as a natural boundary to fluid circulation. Similar behavior is observed near the intrusive bodies. In each geological section the fluid flow shows a particular behavior (see Figure 6 for location).

In section B-B' (Figure 15), the water circulation systems show an advective pattern (*i.e.*, no convective cells are observed). The only surficial expression of the fluid circulation is the salt concentration, which agrees with the observed total dissolved solids.

In section C-C' (Figure 16) an advection pattern is also observed. However, one convective cell occurs near the coast-

Table 1

Petrophysical values used to simulate seawater intrusion at the Costa de Hermosillo aquifer.

Code	Lithology	Hydro-stratigraphy	Permeability		Porosity %	Dispersion coefficient (m ² /s)
			in x k (m ²)	in y		
L1	Continental clast	gravel, sand, limes and clays	1.10 ⁻¹⁸	1.10 ⁻¹⁸	10	4.10-6
L2	Marine clays	impervious marine clays	5.10 ⁻¹⁷	5.10 ⁻¹⁷	17	6.10-6
L3	Igneous rocks	fractured igneous rocks	4.10 ⁻¹²	1.10 ⁻¹²	19	6.6.10-6
L4	Marine clast	carbonated rocks and marine clast	4.10 ⁻¹²	1.10 ⁻¹³	17	6.6.10-6
L5	Basement	granitic and metamorphic rocks	1.10 ⁻¹⁹	1.10 ⁻¹⁹	1	1.10-6

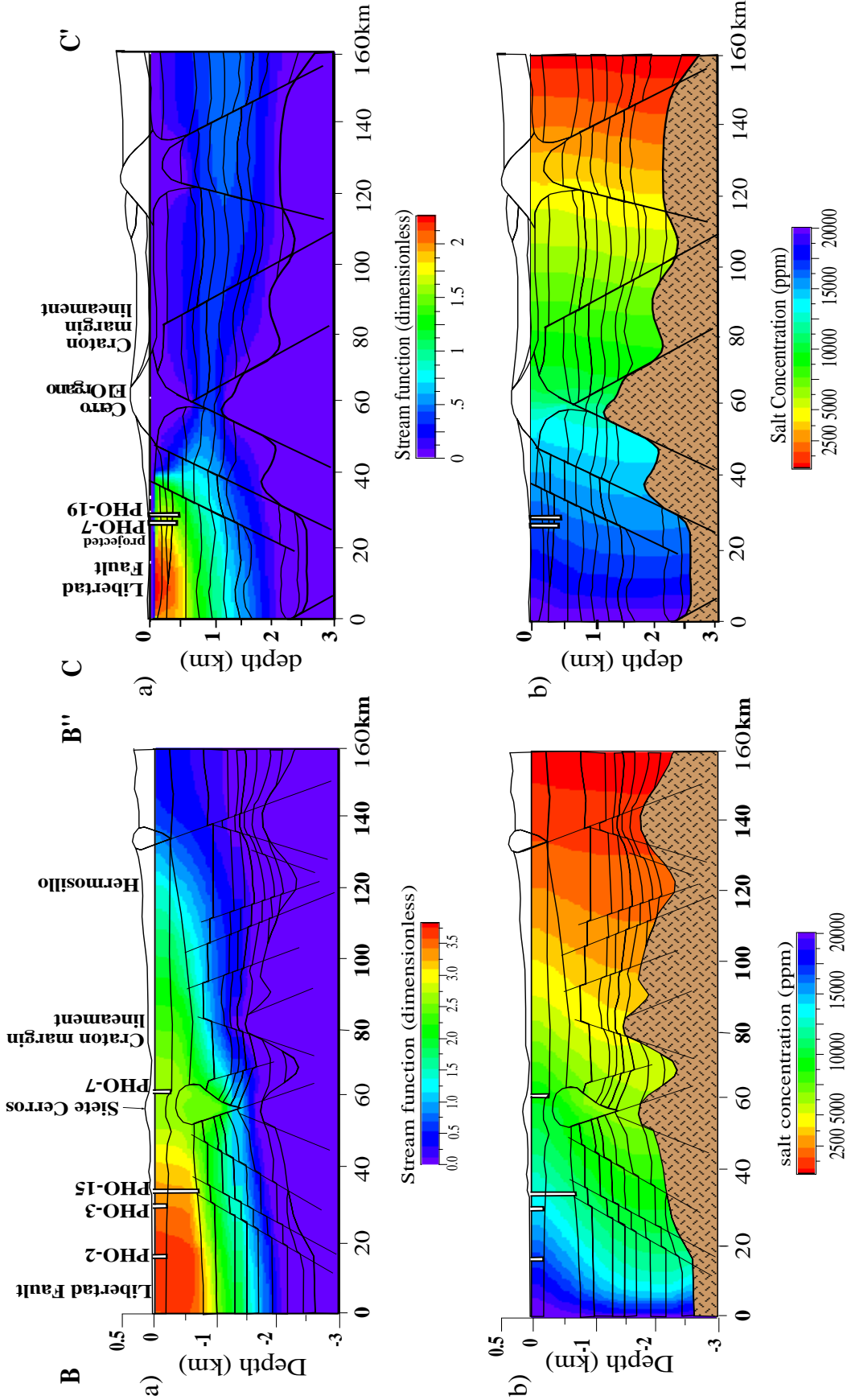


Fig. 15. Results of the numerical simulation for B-B' geological profile. (a) Fluid flow, (b) Total dissolved solids concentration (ppm). See Fig. 6a for location.

Fig. 16. Results of the numerical simulation for C-C' geological profile. (a) Fluid flow, (b) Total dissolved solids concentration (ppm). See Fig. 6a for location.

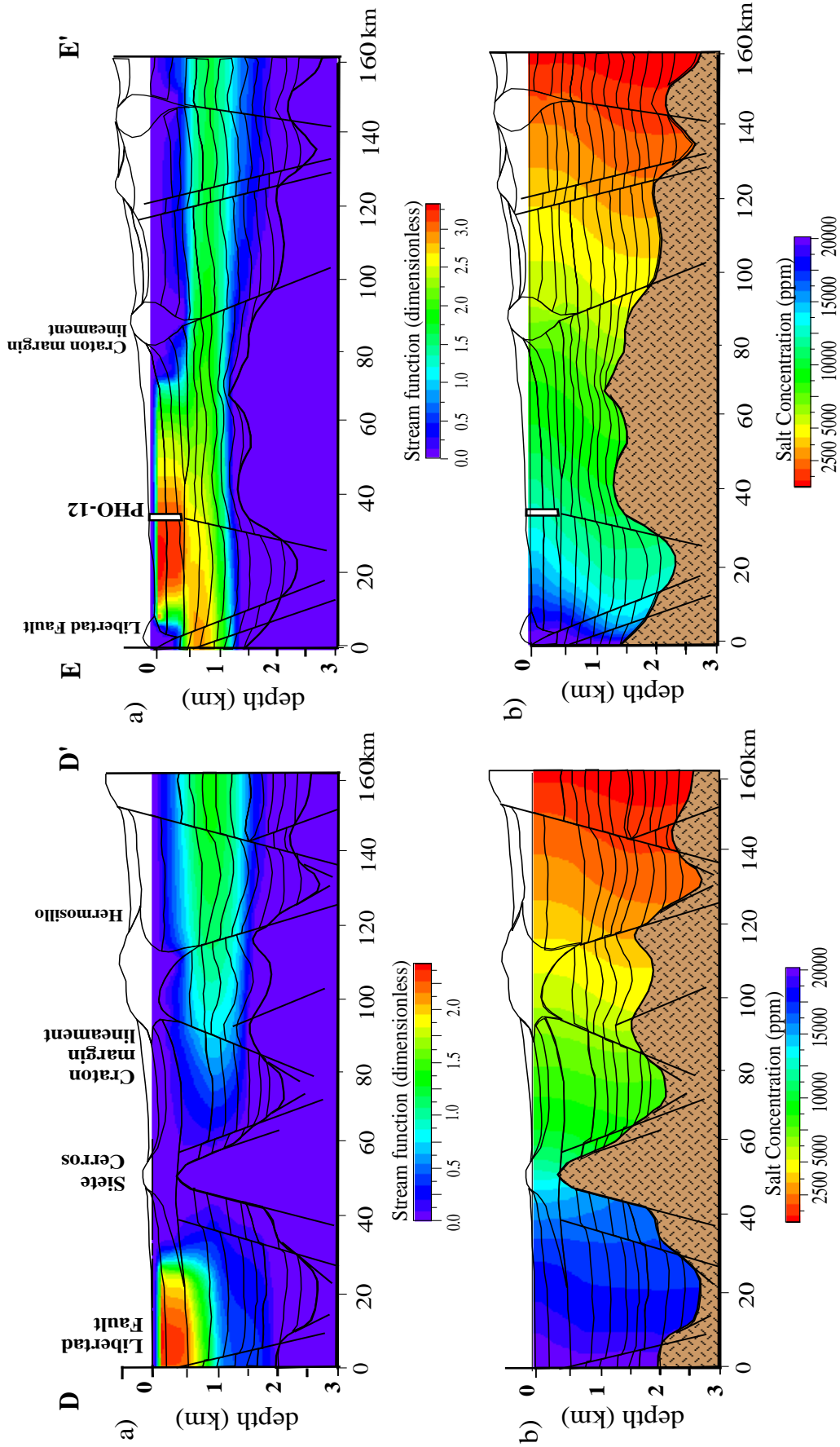


Fig. 17. Results of the numerical simulation for D-D' geological profile. (a) Fluid flow, (b) Total dissolved solids concentration (ppm). See Fig. 6a for location.

Fig. 18. Results of the numerical simulation for E-E' geological profile. (a) Fluid flow, (b) Total dissolved solids concentration (ppm). See Fig. 6a for location.

line. This last convective cell is indicative of an important barrier to the salt intrusion; it explains why we have a smaller salt concentration in this profile.

In section D-D' (Figure 17), two convective cells are observed: one near the coastline, permitting recirculation of the salt to the sea, and the other maintaining freshwater to the left of the intrusive body.

In section E-E' (Figure 18) one advective pattern is observed, with minor convective cells near the surface. Here we clearly observed the important effect of intrusives outcropping at the surface. These intrusives restrain the circulation of fluids in the region between them. Thus the saltwater intrusion only affects the first 30 km and the freshwater to the left of the section is practically unaltered.

We compared the measured salt concentrations at pumping wells with that obtained from our numerical simulations. Under the present exploitation regime, the front of the seawater intrusion is predicted to be located 40 km inland and the salt concentration to exceed 5000 ppm, in agreement with the observed data.

CONCLUSIONS

The depth to the basement, obtained by inversion of gravity data, ranges from 300 to 3500 m. To the E and N of Hermosillo the basement features N-S structures. In the second and third geological subprovinces of Gastil and Krummenacher (1977) the lineaments have a NE-SW orientation. In the same domains the Libertad fault and the other linear tectonic features correlate with the NW-SE Cerro Prieto lineaments. A series of structural highs alternates with structural lows. Several of the structural lows are interconnected, allowing the flow of seawater inland. The structural highs act as barriers to the underground seawater flow. Between Hermosillo and Kino Bay, the basement constitutes a subcircular structural high. The total dissolved solids in this area present a subcircular pattern that correlates with the structural high.

Vertical electric soundings helped us locate the seawater intrusion front. The front of the seawater intrusion is located more than 25 km inland and is more than 200 m deep. This result implies that the impervious barrier of clays cannot stop the sea intrusion. We integrated the basement topography with all the available information about the geologic column (borehole information, surficial geology, general regional stratigraphic sequence, mapped and inferred faults, electrostratigraphy) and established a geologic model of the aquifer. This geological model was used to numerically simulate the seawater intrusion.

A dimensionless formulation based on (1) Darcy's Law

and (2) continuity of water and of dissolved salt equations, and (3) the constitutive equation relating fluid density to the salt concentration, was used to numerically analyze the seawater intrusion. A finite-difference scheme was used to solve the coupled differential equations. Four geologic profiles were simplified, by clustering or ungrouping the geologic layers. The 160 x 3 km domain of each of the geologic sections was parametrized on a regular grid of 120 x 30 nodes. In general, the parameters such as permeability, viscosity, dispersion, etc. change within a given geological formation from place to place. For the study area there are no direct measurements for these parameters. We made trial simulations changing the values of the parameters, and those values that reproduce the known hydrologic conditions were used in the final simulations.

We assume a high permeability contrast between the basement and its volcanosedimentary cover. We took into account the anisotropy of hydrophysical properties of the layers. The boundary conditions used to solve the system equations were modified depending on the observations, mainly depending of total dissolved solids values and of the hydrological balance.

In general the flow of water is controlled by subsurface structures of the area. The numerical simulation shows that the structural highs act as barriers to the saltwater intrusion.

Freshwater and saltwater mix about 40 km inland, implying that the clay beds are not stopping the seawater intrusion. Our results reproduce fairly well the present salt concentration as found in wells.

ACKNOWLEDGMENTS

We are thankful to the National Water Commission (CNA) who provided the original hydrological data. We thank R. Martínez for his suggestions and comments, and A. Tejero for his support during the field work. We also thank A. García, D. Alatríste and M. A. Maruri and the students of the Field Potential Methods and Electric Prospection courses from the Faculty of Engineering-UNAM, for their enthusiastic help during the field work. Financial support was provided by PAPIIT-DGAPA-UNAM grant No. IN108695.

BIBLIOGRAPHY

- ABDOH, A., D. COWAN and M. PILKINGTON, 1990. 3D gravity inversion of the Cheshire basin. *Geophys. Prospect.* 38, 399-1011.
- ALENCASTER, G., 1961. Estratigrafía del Triásico superior de la parte central del estado de Sonora. *Paleontol. Mex.*, 1-18.

- ANDERSON, T. H. and L. T. SILVER, 1977. U-Pb isotope ages of granitic plutons near Cananea, Sonora. *Econ. Geol.*, 72, 827-836.
- ANDERSON, T. H. and L. T. SILVER, 1981. An overview of Precambrian rocks in Sonora. *Rev. Inst. Geología, UNAM*, 5, 131-139.
- ANDREWS, R. W., 1981. Salt-water intrusion in the Costa de Hermosillo, Mexico: A numerical analysis of water management proposals. *Ground Water*, 19, 635-647 .
- ARREGUIN, J., G. FIGUEROA and S. PEÑA, 1968. Estudio hidrogeológico completo de los acuíferos de la Costa de Hermosillo, Sonora. Ariel Consultores y Dirección de Aguas Subterráneas. Secretaría de Recursos Hídricos, México. vol. 1, 1-18.
- BEAR, J. and G. DAGAN, 1964. Moving interface in coastal aquifers. *Hydr. Div. ASCE.*, 106, 193-200.
- BEAUVAIS, L. and T. E. STUMP, 1976. Corals, molluscs and paleogeography of late Jurassic strata of the Poso Serna region, Sonora, Mexico. *Palaeogeogr., Palaeoclim., Palaeoecol.*, 19, 275-301.
- CRUICKSHANK, C. and R. CHAVEZ-GUILLEN, 1969. Reporte. Ingeniería Hidráulica en México, XXXIII: 31-42.
- FERRASI, M. and A. MARINELLI, 1996. An extended formulation of the integrated finite difference method for groundwater flow and transport. *J. Hydrol.*, 453-471.
- FLORES-MARQUEZ, E. L. 1992. Transfert de chaleur et de masse en milieu sédimentaire et fracturé. Modélisation numérique de la convection naturelle autour du site géothermique de Soultz (Graben du Rhin). Ph. D : Institut National Polytechnique de Lorraine, 229 pp.
- FLORES-MARQUEZ, E. L., 1998. Two Dimensional Solute transport model in an Anisotropic and Heterogeneous Porous Medium. In preparation.
- DE LA FUENTE, D.M., C.L. AIKEN, J.M. MENA and R. W. SIMPSON, 1994. Cartas gravimétricas de la República Mexicana. Instituto de Geofísica, UNAM, México D.F.
- GASTIL, R. G. and D. KRUMMENACHER, 1977. Reconnaissance geology of coastal Sonora between Puerto Lobos and Bahía Kino. *Geol. Soc. Amer. Bull.*, 88, 189-198.
- GHASSEMI, F., A.J. JAKEMAN, G. JACOBSON and K.F. HOWARD, 1996. Simulation of seawater intrusion with 2D and 3D models: Nauru Island case study. *Hydrogeol. J.*, 4, 4-22.
- GIPOULOUX, O., J.-P. CALTAGIRONE and P. MOREL, 1991. Approche numérique du comportement de la loi de Darcy en fonction du nombre de Reynolds. Comptes Rendus de l'Académie des Sciences (Paris), Série II, 313: 1493-1498.
- GOMEZ, J. 1971. Sobre la presencia de estratos marinos del Mioceno en el estado de Sonora, México. *Rev. Inst. Mexicano del Petróleo*, 3, 77-78.
- GRANT, F. S. and G. F. WEST, 1965. Interpretation theory in applied geophysics. New York, 584 pp.
- HENRY, H. R., 1959. Salt Intrusion into Freshwater Aquifers. *J. Geophys. Res.*, 64, 1911-1959.
- HENRY, H. R., 1964. Effect of dispersion on salt encroachment in coastal aquifers. In: H.H.C. et al. (Editors), Sea Water in Coastal Aquifers. US Geological Survey Water, Supply Paper, pp. 1613-C.
- KING, P. B., 1939. Geologic Reconnaissance in northern Sierra Madre Occidental of Mexico. *Geol. Soc. Amer. Bull.*, 50, 1624-1722.
- LEE, C.-H. and R. T.-S. CHENG, 1974. On Seawater Encroachment in Coastal Aquifers. *Water Resour. Res.*, 10, 1039-1043.
- MERRIAM, R., 1972. Reconnaissance geologic map of the Sonoyta quadrangle, northwest Sonora, Mexico. *Geol. Soc. Amer. Bull.*, 83, 3523-3536.
- MUALEM, Y. and J. BEAR, 1974. The shape of the interface in steady flow in a stratified aquifer. *Water Resour. Res.*, 10, 1207.
- O'NEILL, D. J., 1975. Improved linear filter coefficients for application, in apparent resistivity computation. *Bull. Aust. Soc. Explor. Geophys.*, 6, 104-109.
- PARKER, R. L., 1973. The rapid calculation of potential anomalies. *Geophys. J. Royal Astron. Soc.*, 31, 447-455.
- PILKINGTON, M. and D. J. CROSSLEY, 1986. Determination of crustal interface topography from potential fields. *Geophysics*, 51, 1277-1284.
- PINDER, G. F. and H. H. A. COOPER, 1970. A numerical technique for calculating the transient position of the saltwater front. *Water Resour. Res.*, 6, 875.

- RANGIN, C. 1978. Consideraciones sobre la evolución geológica de la parte septentrional del estado de Sonora. Libroto Guía del Primer Simposio Sobre la Geología y Potencial Minero del estado de Sonora. Inst. de Geología, UNAM, 35-56.
- RANGIN, C., 1981. Late Triassic to Late Cretaceous geological evolution of northwestern Mexico: 77th annual international meeting of the Geological Society of America, Geol. Sur. of America,
- SEGOL, G. and A. G. F. PINDER, 1976. Transient simulation of saltwater intrusion in south-eastern Florida. *Water Resour. Res.*, 12, 65.
- SEGOL, G., G. F. PINDER and W. G. GRAY, 1975. A Galerkin finite element technique for calculating the transient position of the saltwater front. *Water Resour. Res.*, 11, 343.
- SHAMIR, U. and G. DAGAN, 1971. Motion of sea water interface in coastal aquifers: A numerical solution. *Water Resour. Res.*, 7, 644.
- STEINICH, B., I. SIMON, J. A. CHAVARRIA and L. E. MARIN, 1997. Geophysical investigations of the vadose zone in the Valley of Hermosillo aquifer, Sonora, Mexico. *Geofis. Int.*, 36, 191-200.
- WOOLLARD, G. P., 1979. The new gravity system changes international gravity base values and anomalies. *Geophysics*, 44, 1352-1366.
-
- Flores-Márquez, E.L., J.O. Campos-Enríquez, R.E. Chávez-Segura and J. A. Castro-García
Instituto de Geofísica, UNAM,
Coyoacán, 04510 México D.F., México.